

IDŐJÁRÁS

Quarterly Journal of the Hungarian Meteorological Service
Vol. 125, No. 1, January – March, 2021, pp. 151–166

Synoptic aspects associated with pervasive dust storms in the southwestern regions of Iran

Mahdi Sedaghat^{1,*}, **Hasan Hajimohammadi**², and **Vahid Shafaie**³

¹*Department of Geography
Payame Noor University(PNU), Tehran, Iran*

²*Tarbiat Modares University, Tehran, Iran*

³*University of Tehran, Tehran, Iran*

**Corresponding author E-mail: sedaghat.me@pnu.ac.ir*

(Manuscript received in final form March 24, 2020)

Abstract— Dust storm is a natural hazardous phenomenon that affects arid and semi-arid regions of the world the same as Iran. The present research aims to investigate the formation of synoptic patterns of pervasive dust storms (PDSs) in the southwestern regions of Iran. For this purpose, daily data of visibility less than 1000m in 16 synoptic stations (Ilam and Khuzestan provinces) were reviewed during 2004–2017, and 59 PDSs with more than 2 days of duration (overlapped: 70% of the region) were extracted. In practice, mid-level atmospheric data (500, 700, 850 hPa, and sea level pressure (SLP)) with 2.5*2.5 degree resolution (domain: 0-80°E and 10-70°N) were obtained from NCEP/NCAR reanalysis dataset, and the matrix 825*59 of 500 hPa data was performed. Principal component analysis (PCA) with S-mod, were used for extracting synoptic patterns that make PDSs. PCA showed that the first four components ensured more than 86.45% of the data variance. PDSs classification based on output components showed that the patterns had seasonal structures. Synoptically, the north wind blowing in the first pattern is the most dominant structure in the formation of PDSs in the Middle East. The second and third patterns showed postfrontal structures. The fourth pattern with prefrontal structure was the reason for PDSs in the cold seasons of the year. From the four final patterns, the first three patterns showed the dominance of the Persian trough in the SLP maps. Mean values map analysis of the aerosol optical depth suggests that each of the most consistent synoptic patterns stimulates special dust centers.

Key-words: pervasive dust storms, synoptic climatology, PCA, persian trough, Iran

1. Introduction

Dust emissions play an important role in the weather, bio-cycle, and other systems of the Earth (*Choobari et al.*, 2014; *Mahowald et al.*, 2014), which could disturb the general health and economic activities (*Raviand D'Odorico*, 2005) and lead to soil erosion (*Warren*, 2014) by damaging the vegetation (*Tegen et al.*, 2004). The climate of storm dust has been well documented by various researchers through synoptic analysis of the past 50 years in Asia (*Sun et al.*, 2001; *Zhou*, 2001; *Chun et al.*, 2001; *Qian et al.*, 2002; *Natsagdorj et al.*, 2003, *Kurosaki and Mikami*, 2003; *Shao and Wang*, 2003). Different atmospheric phenomena lead to the occurrence of dust events at synoptic, regional, and local scales. Dust emission is intensified by some of the synoptic meteorological patterns such as the identified frontal and synoptic systems (*Trigo et al.*, 1999, 2002). The statistical results of 28 spring dust events that occurred during 2015–2018 showed that all of these dust storms were triggered by mogul cyclones or Asian highs (*Li et al.*, 2019). In western Asia, most of these phenomena are observed in one of the three subgroups, including north wind, frontal systems, and convective systems (WMO, 2013).

In a study conducted by *Khoshkish et al.* (2011), the atmosphere middle-level depression, low-pressure systems in the Persian Gulf region, and the stream resulted from temperature difference between the east of Turkey and north west of Iraq toward the Persian Gulf were identified as the main factors in transferring dust to the west of Iran. High pressure in the middle level of the atmosphere and immigrant systems of west winds are the most critical synoptic factors affecting the dust phenomenon in the Middle East, and these depressions and immigrant cyclones penetrate to the region when the subtropical high pressure is absent or weak (*Zolfaghari and Abedzadeh*, 2005). In another research by *Zolfaghari et al.* (2012), the convergence of the middle-level high-pressure systems, thermal low-pressure systems, and increase of pressure gradient in the days of peak activity of dust events were identified as the reasons of reinforcing high-level wind systems and transferring and emitting huge amounts of fine dusts in vast sections of eastwest, west and northwest of Iran.

In the warm period of the year and at the end of a cold period of the year and transition months (spring and autumn), thermodynamic and dynamic processes play an essential role in the formation and transfer of dust to the west of Iran, respectively (*Azizi, et al.*, 2012). Besides, a meteorological pattern called the Persian Gulf's thermal low-pressure ridge, and penetration of European high-pressure ridge on the Red Sea, and the passage of the Mediterranean Trough's middle-level waves above the northwest of Iraq and east of Syria were emphasized by *Ghahri et al.* (2012). The synoptic analysis of 19 PDSs in Khuzestan province with a duration of two days provided four general patterns (*Lashkari and Sabouri*; 2013). In a study by *Babaei et al.* (2016), by isolating the frequency of dust incidents in two warm and cold

periods of the year in the western half of Iran, the dominant synoptic patterns of their occurrence were interpreted.

Several case studies on dust storms in western countries of Asia have been conducted. From among these studies, analysis of the great dust storm in Saudi Arabia in March 2009 was done by *Alharbi et al.* (2012), and it was showed that this storm happened due to the passage of a cold front by emitting an intense upstream jet current. Furthermore, analysis of the meteorological reasons of an unprecedented pervasive dust after the occurrence of a lightning storm in Qatar and around the Middle East in February 4, 2010 showed, that the cold weather above Saudi Arabia began a northwest wind which led to the dust storm in some sections of the Arabian Peninsula (*Monikumar and Revikumar*; 2012). The 850 hPa level was introduced by *Abdul-Wahab et al.* (2017) as the criterion of studying changes in the pressure's synoptic patterns to study the seasonal changes of dust in the east and west of Saudi Arabia.

Nowadays, some researchers have turned to study indices such as aerosol optical depth (AOD) to study synoptically the dust phenomena using remote sensing technology (*Qi et al.*, 2013; *Alam et al.*, 2014). In this regard, *Namdari et al.* (2016) analyzed the spatiotemporal analysis of AOD index values in western Iran. The increase of dust storms' frequency during the past years has introduced this natural hazard as the most important biological threat in the western half of Iran. Thus, identification of synoptic climatic behavior of these events makes it possible to predict the origin, performance mechanism, and evaluation of measures to reduce their possible damages. In this regard, researchers attempted to study the dominant mechanisms leading to PDS in the west of Iran using a synoptic modeling method. In this area, the wind flow tracking was emphasized by studying synoptic maps for identifying and monitoring the route of dust storms (*Vali et al.*, 2014).

2. Data and methodology

A dust storm, also called sandstorm, is a meteorological phenomenon common in arid and semi-arid regions. Dust storms arise when a gust front or other strong wind blows loose sand and dirt from a dry surface. Sand and dust storms usually occur when strong winds lift large amounts of sand and dust from bare, dry soils into the atmosphere (*Nickovic, et al.*, 2015). Visibility can be used as a dust weather indicator that recorded in regular weather observations metrically (*Wang*, 2015).

In this research, using visibility less than 1000m daily data of 16 synoptic stations located at Khuzestan and Ilam provinces during the period 2004–2017 (*Fig. 1*), PDSs with more than two days duration in more than 70% of stations in the region were extracted.

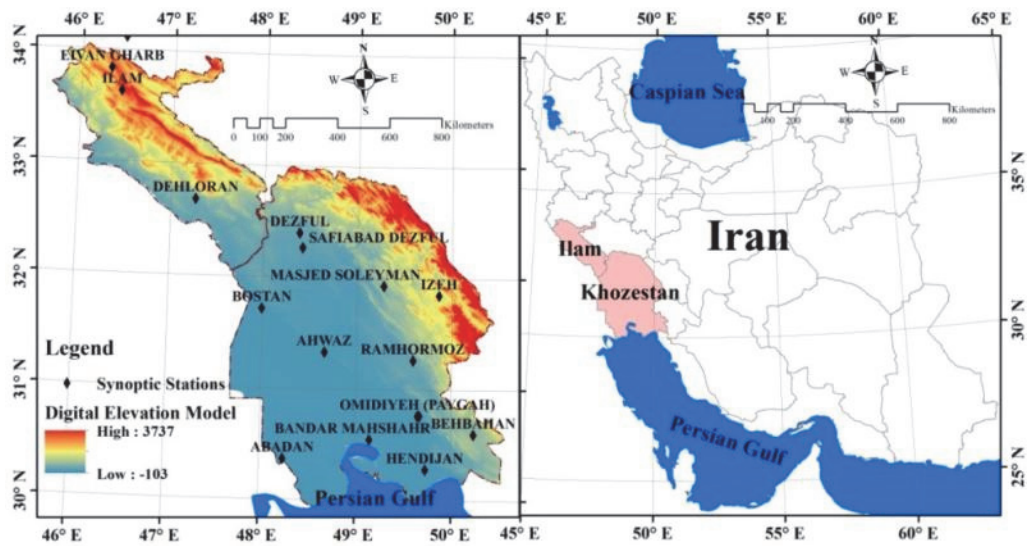


Fig. 1. The region under study and the location of synoptic stations.

Then, by establishing the mid-level atmospheric databases with 2.5×2.5 degree resolution (domain: $0-80^\circ\text{E}$ and $10-70^\circ\text{N}$, Fig. 2), data were extracted from levels 500, 700, 850 hPa, and SLP of 59 selected pervasive dust events and the matrix 825×59 of 500 hPa data was performed.

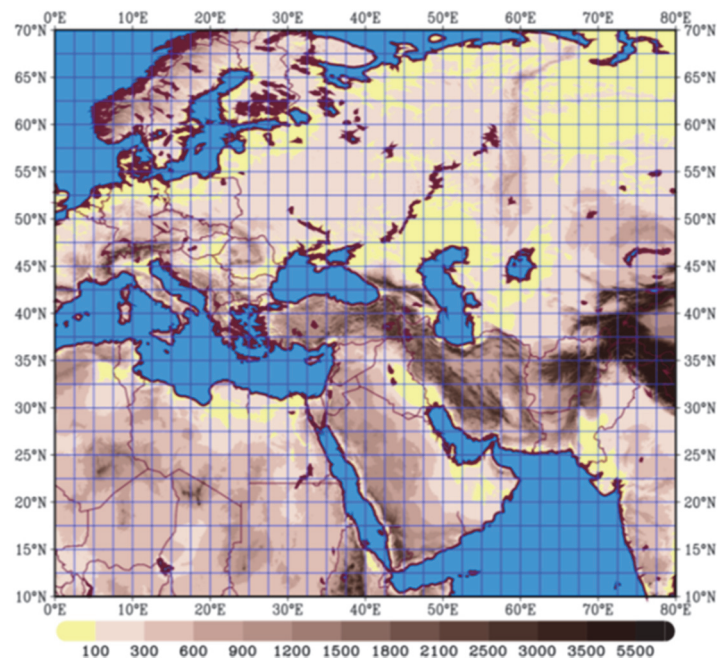


Fig. 2. The area of mid-level atmospheric data.

In the following, to find the patterns for creating dust phenomena, principal component analysis (PCA) was used. The principal component analysis (PCA) is probably the most popular multivariate statistical technique, and it is used by almost all scientific disciplines (Abdi and Williams, 2010). Its goal is to extract the important information from the table, to represent it as a set of new orthogonal variables called principal components, and to display the pattern of similarity of the observations and variables as points in maps. One of the applications of PCA in synoptic climatology is the map-pattern classification.

In this method, after the preparation of data, the investigator selects the mode decomposition, type of dispersion matrix, and type of analysis. The PCA-based map-pattern classification targets the main modes of spatial variation of just one variable; usually surface pressure or geopotential height. Therefore, the mode decomposition and the type of dispersion matrix are S-mode and correlation matrix, respectively. PCA produces component loading and component-scores matrices, with the m principal components corresponding to the N data points on the map. The investigator applies a clustering algorithm to the scores matrix to identify the most common combinations of principal-component scores. However, the PCA with S-mode enables the analysis of patterns without cluster analysis (Raziei, 2018).

Furthermore, using the global aerosol database for MODIS Global Studies Group*, the aerosol optical depth index† was extracted for each of the patterns to show the performance of the system and the rise of dust from the level of possible centers. The aerosol optical depth can be considered as an index of dust events so that in dust storms, the index values are changed from 0.5 to 3, and when value 5 is reached, PDS is formed (Legrand *et al.*, 2001).

3. Results

The monthly and seasonal frequencies of 59 identified PDSs showed that the highest number of events was related to July with 14 days (Fig. 3). After that, May with 10 days got the second rank. Seasonally, spring and summer both with 20 days had the highest numbers of PDSs. Winter (especially March) and autumn were placed in the next ranks with a total of 14 and 5 events, respectively.

* This base provides the aerosol optical depth based on the blue spectrum depth algorithm with spatial resolution of 10 km (Hsu *et al.*, 2004).

† The aerosol optical depth value dependent on wavelength is defined as the light reduction in the length unit on a specified route (Charlson and Heintzenberg, 1995).

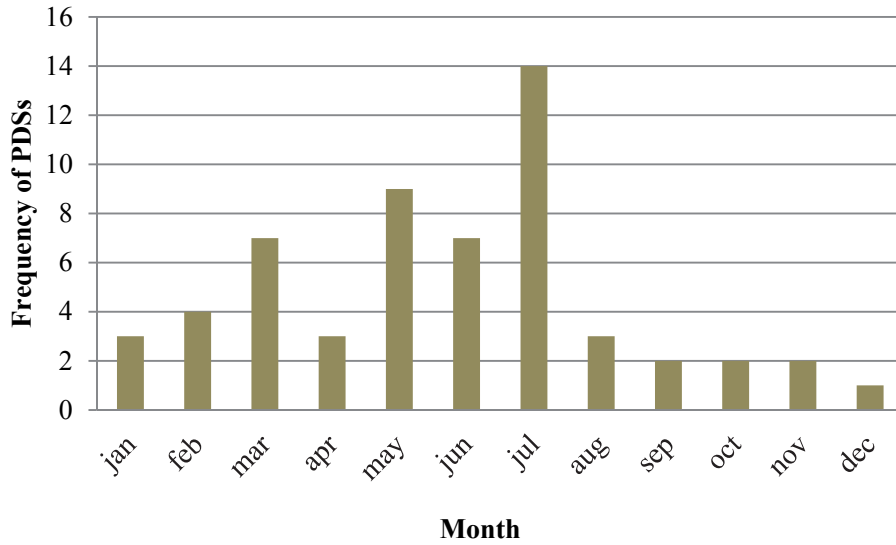


Fig. 3. The monthly frequency of PDSs in the west of Iran during 2004-2017.

After performing the PCA, the components that explained more than 5% of the variance of the data were selected as the final components (*Kaiser, 1960*). However, PCA showed that the first 4 components justify more than 86.45% of data variance (*Fig. 4*). The first component justifies more than 67.3% of this dispersion. The rest of the data dispersion is justifiable, on the other hand.

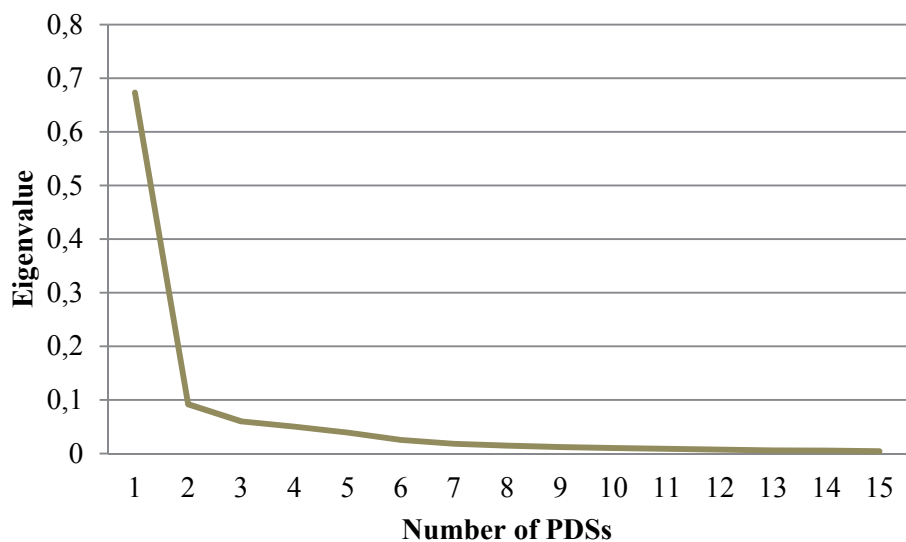


Fig. 4. Scree Plot for PCA

Adjustment of date of PDSs, which have the highest convergence with four synoptic patterns made it possible to analyze the monthly frequency of patterns leading to these events (*Fig. 5*). Results showed that Pattern2 completely was observed summer, so that 74% and 26% of cases occurred in July and two months of August and September, respectively. Pattern1 occurred in winter and somehow in spring: 27% of its cases happens in the last month of the year. 60% of cases in Pattern3 were observed in May, indicating that the desired pattern occurred in spring. Rare cases were observed in the cold period of the year, especially in autumn. Studies showed that the highest frequency of Pattern4 is related to the cold period of the year, which of course showed a 42% frequency in June.

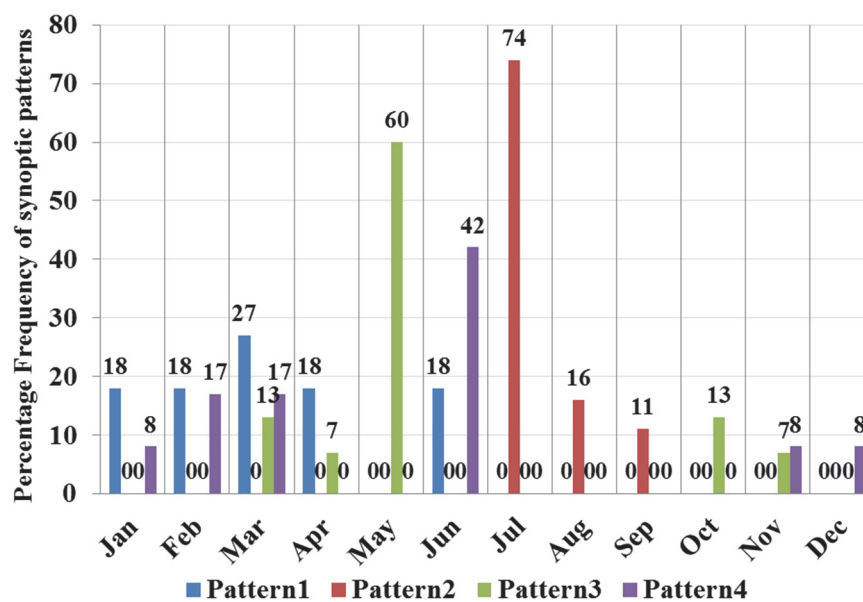


Fig. 5. Monthly frequency of synoptic patterns leading to PDSs in the southwestern regions of Iran during 2004–2017.

Then, the maps extracted from the average level of 500 hPa, stream direction and surface vorticity of 700 hPa, speed and direction of the stream at the 850 hPa level, as well as the SLP relating to all of the four final patterns, were synoptically interpreted.

3.1. Pattern1

According to a low-height field in northern Europe, the relatively low-height ridge above Turkey, and the high-height strong cell above the Arabian Peninsula, an extensive negative vorticity was formed above the Arabian Peninsula and on the southeast and northwest regions of Iran in contrast to the strong positive vorticity

above Turkey, which is obvious at levels 500 and 700 hPa (Fig. 6a,b). Development of the Persian trough according to the northwest-southeast trend of Zagros Mountains at the 850 hPa level and establishment of a low-pressure cell with the central curve of 1000 hPa above Oman and a high-pressure cell with the closed curve of 1010 hPa at the sea level with a pressure difference of 10 hPa led to the creation of a winter north wind in the region by the extensive northwest-southeast stream (Figs. 6c,d). The north wind is the most dominant structure for the creation of extensive dust in the Middle East (Middleton, 1986).

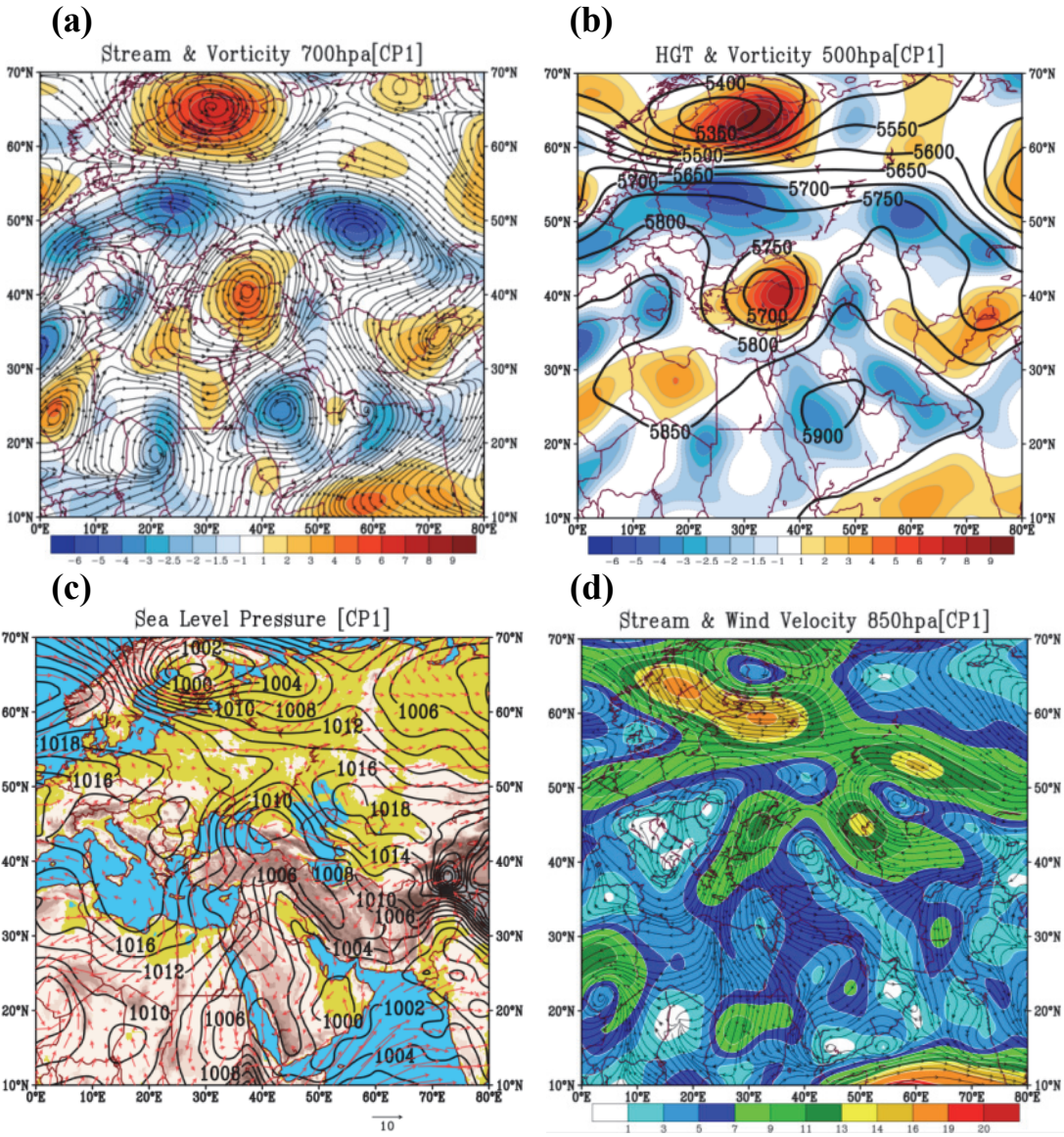


Fig. 6. Meteorological pattern: geo-potential height and vorticity of 500 hPa (a), stream direction and vorticity of 700 hPa (b), stream speed and direction of 850 hPa (c), and SLP (d) from Pattern1.

3.2. Pattern2

At the 500 hPa level of this pattern, we face a low-height system above Russia which sent a ridge toward the Mediterranean Sea and the east of Baikal Lake (Fig. 7a). This structure at the 700 hPa level led to the creation of a positive vorticity core along the Zagros Mountains at the border of Iran and the north of Iraq (Fig. 7b). The high-pressure cores located at the west of the Red Sea and the Arabian Peninsula with a strong low-pressure core above the Persian Gulf led to the creation of a western-eastern wind stream with a high speed in the central and eastern parts of Saudi Arabia up to the border of Iraq along with a summer north wind (Figs. 7c,d).

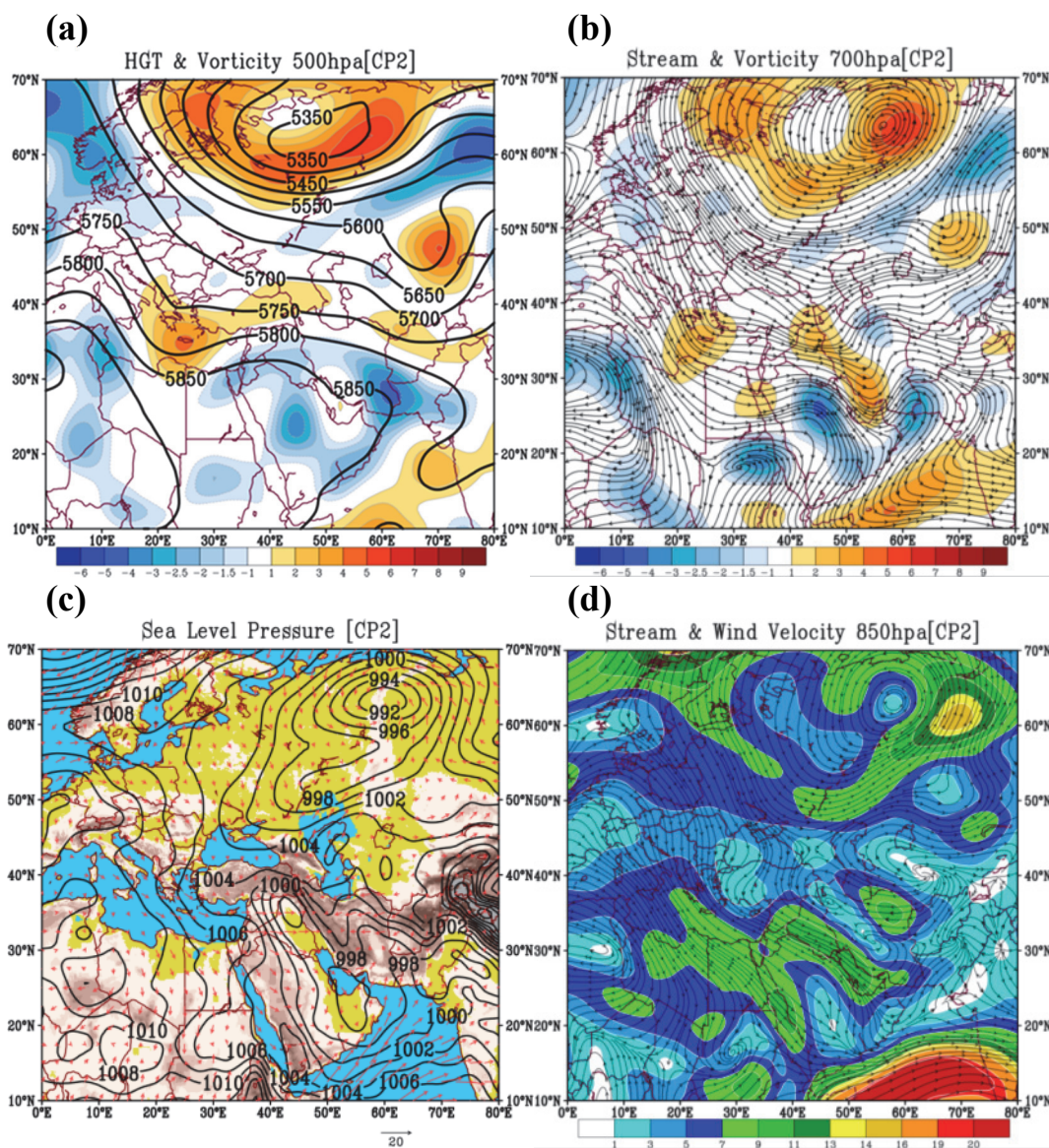


Fig. 7. Meteorological pattern: geopotential height and vorticity of 500 hPa (a), stream direction and vorticity of 700 hPa (b), stream speed and direction of 850 hPa (c), and SLP (d) from Pattern2.

3.3 Pattern3

At the 500 hPa level, the low-height system above northern Europe and the high-height system above Russia are shown which sent the low-height ridge toward the Black Sea and emitted it up to the center of the Mediterranean Sea. In lower widths and higher heights, the subtropical ridge with the curve of 5900 m was sent to northern Africa, the Arabian Peninsula, and up to the western and central parts of Iran (Figs. 8a,b). The expansion of the Persian trough in the form of the low-pressure ridge from the Indian to the Black Sea coast is seen at the levels of 850 hPa and 1000 hPa (Figs. 8c,d).

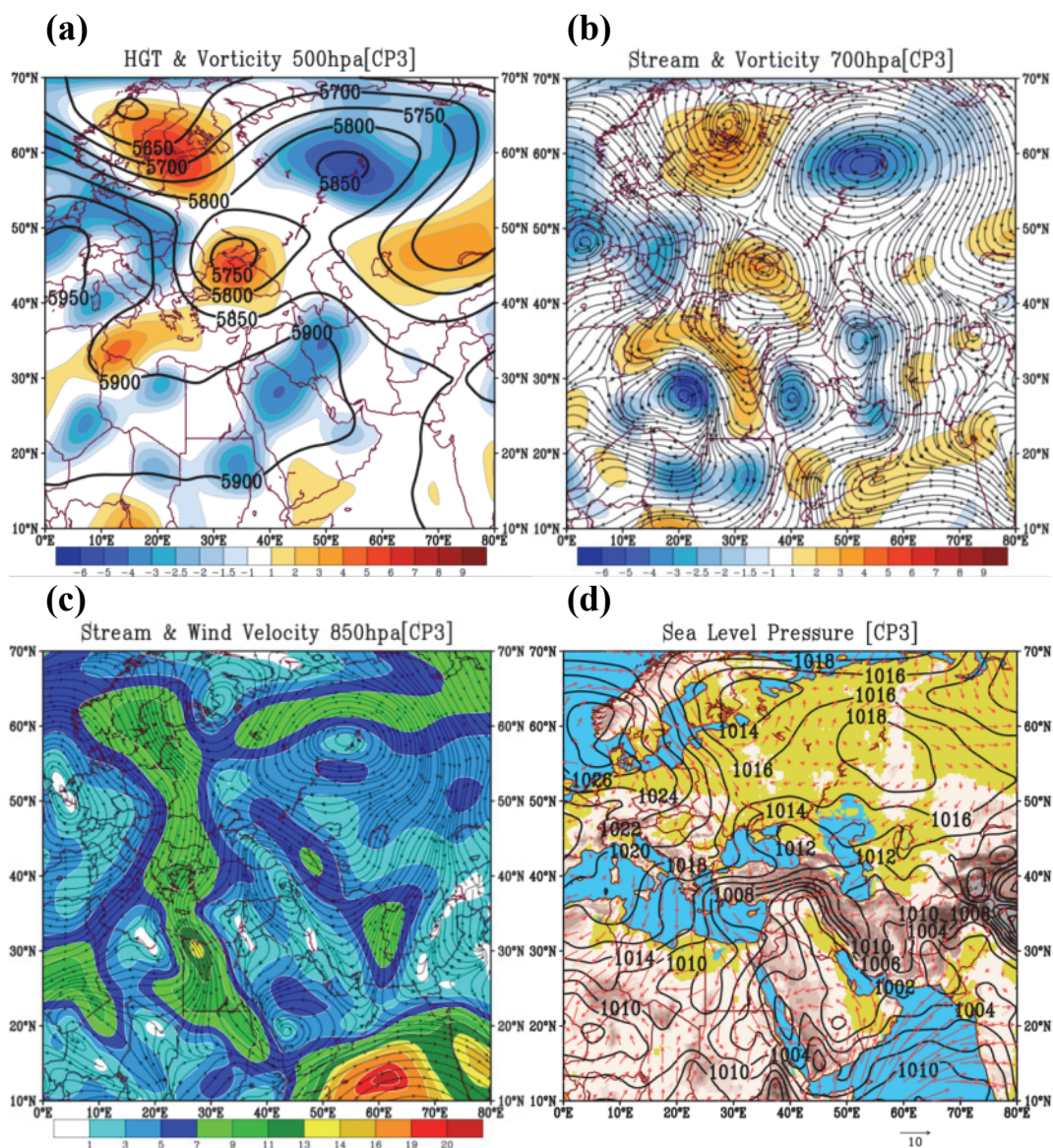


Fig. 8. Meteorological pattern: geopotential height and vorticity of 500 hPa (a), stream direction and vorticity of 700 hPa (b), stream speed and direction of 850 hPa (c), and SLP (d) from Pattern3.

3.4. Pattern4

This pattern at the 500 hPa level shows a low-pressure ridge of an immigrant system in the cold period of the year. In eastern Europe and the Arabian Peninsula, a strong high-height cell and ridge became dominant respectively, and a low-height ridge was formed between these two above the eastern part of the Mediterranean Sea. This structure has led to relatively strong vorticity above the eastern part of the Mediterranean Sea at the 500 and 700 hPa levels (Fig. 9a,b). The encounter of subtropical jet and polar jet at levels 500 and 700 hPa was evident, leading to the orbital circulation and the maximum wind speed at the 850 hPa level in the border regions of Iran, Syria, and northern parts of Saudi Arabia (Fig. 9c). The sea-level high pressure above the northern and central parts of Iran with various cores led to the stability of the dust mass (Fig. 9d).

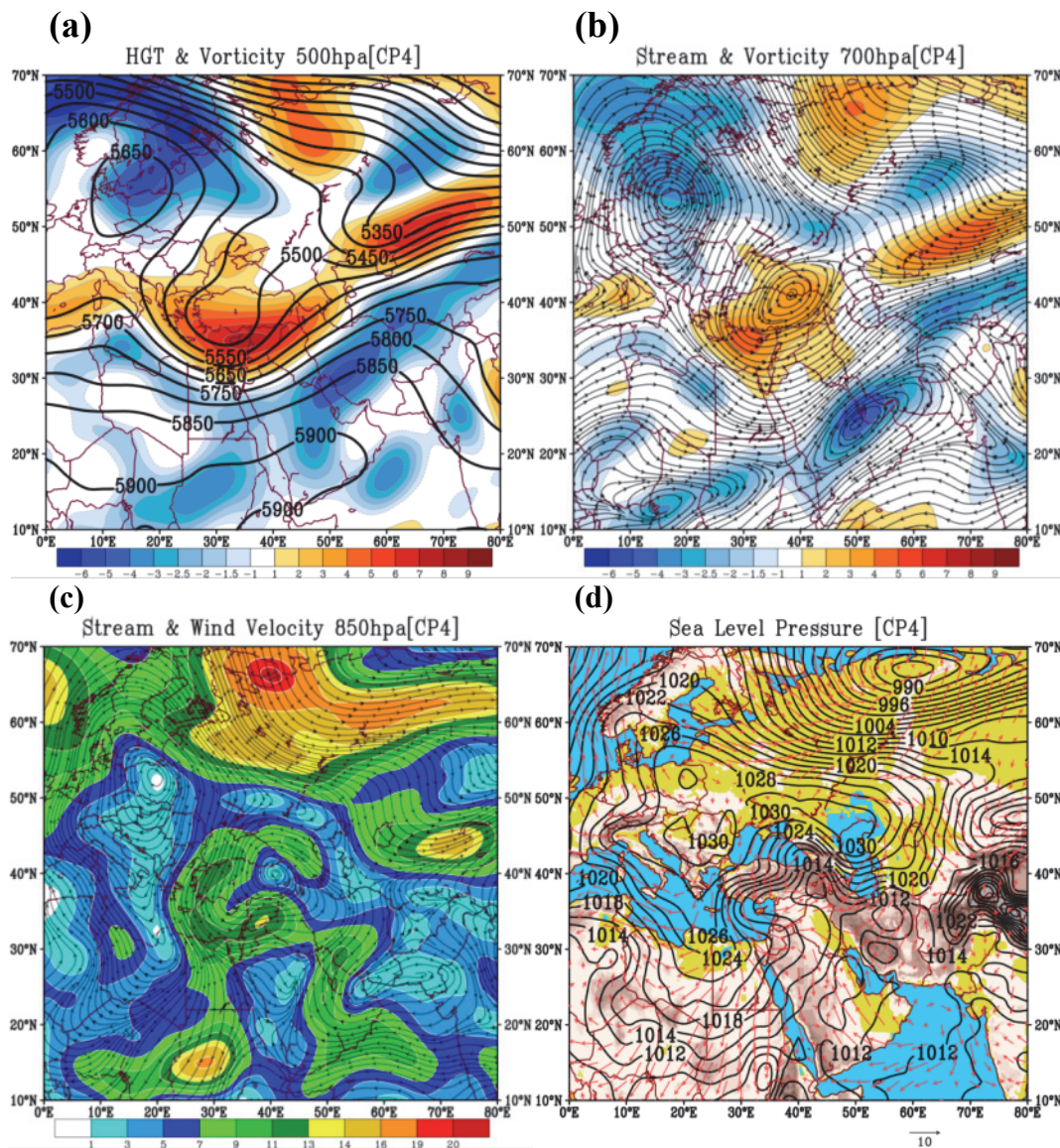


Fig. 9. Meteorological pattern: geopotential height and vorticity of 500 hPa (a), stream direction and vorticity of 700 hPa (b), stream speed and direction of 850 hPa (c), and SLP (d) from Pattern4.

Finally, mean values analysis of AOD maps estimated of the each most consistent synoptic patterns showed that in Pattern1 (Fig. 10a), the north wind stream in the northwest-southeast direction led to the rise of dust from the Mesopotamian plains all around Iran, Syria, and lagoons such as Hoor-al-Azim in Iran. Pattern2 (Fig. 10b) also stimulates dust centers in the western, central, and eastern of Saudi Arabia by intensifying the western-eastern wind stream. Despite its similarity in appearance with Pattern2, Pattern3 (Fig. 10c) affects dust centers in the border between Iraq and Syria due to its location at higher latitude. However, Pattern4 (Fig. 10d) led to the rise of dust in these regions by creating a stream with the maximum wind speed on dust centers in the border between Iraq, Syria, and the eastern parts of Saudi Arabia.

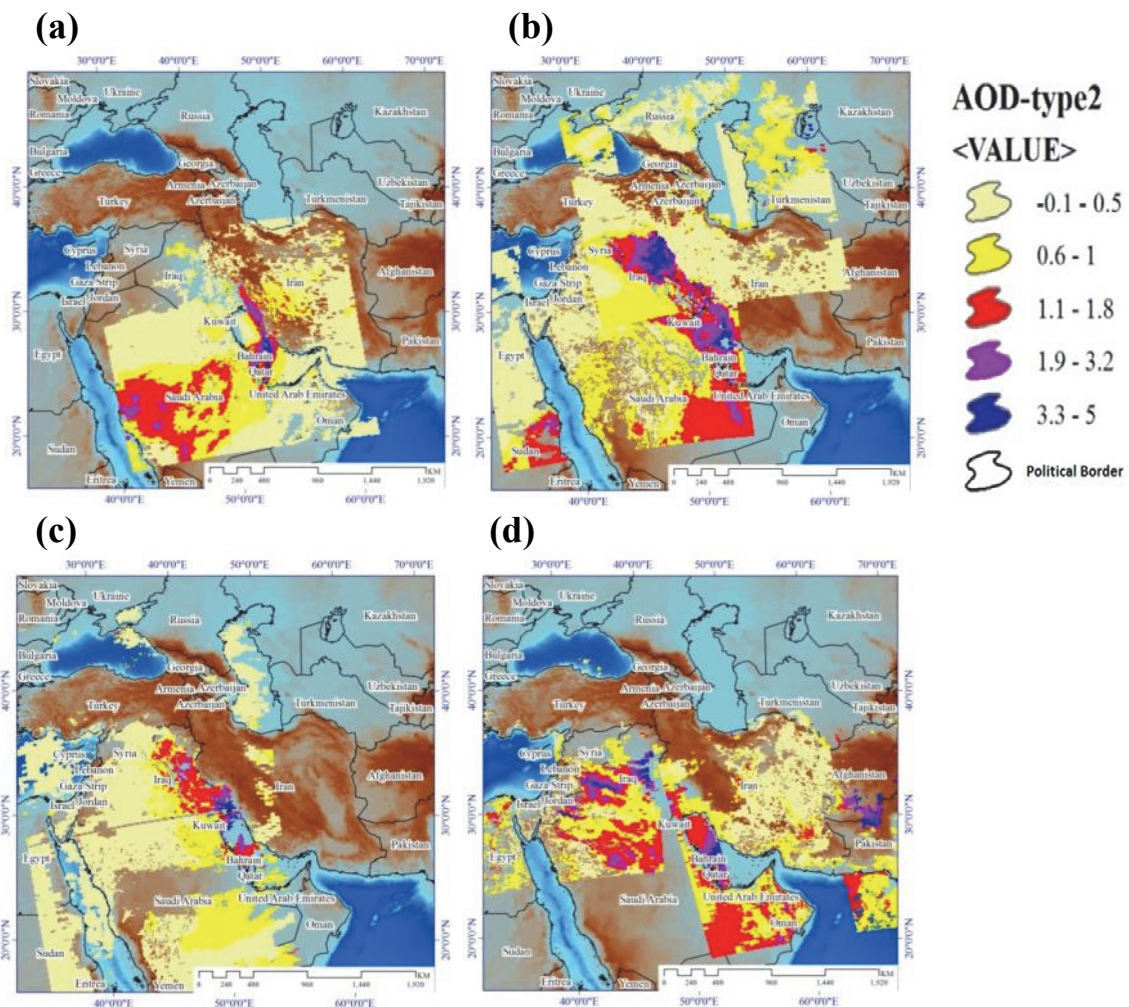


Fig. 10. The average aerosol optical depth index in patterns 1(a), 2(b), 3(c), and 4(d). The optical depth of less than 0.1 shows clear weather and the optical depth of more than 4 presents the density of aerosols.

4. Conclusion

Dust storms are natural hazards which have a significant effect on the arid and semi-arid areas of the world, including Iran (*Sedaghat et al.*, 2016). The frequency analysis of 59 pervasive dust storms (PDSs) in the west of Iran showed that the warm period of the year, especially July with 14 events had the highest frequency. The principal component analysis showed that the first 9 components justified more than 93.5% of the data variance. From among four final patterns resulted from cluster sampling, three patterns showed the dominance of the Persian trough in the SLP map. The Persian trough indicates the formation of a summer atmosphere in the region of the Mediterranean Sea (*Sedaghat and Nazaripour*; 2018).

As *Li et al.* (2019) emphasize on the Gobi Desert in China, cyclonic synoptic systems have been the main cause of dust storms in desert areas. Dust storms resulted from north winds and matched with Pattern1 in the present research by forming high pressure above the northern part of Saudi Arabia, low pressure above Afghanistan, and thermodynamic low-pressure ridge of the Persian Trough relating to the monsoon locating above the southern part of Arabian Peninsula have led to the creation and stream of north winds above the Persian Gulf. The presence of this trough at 850 hPa level was confirmed by *Lashkari and Sabouri* (2013).

Postfrontal dust storms matched with patterns 2 and 3 are formed above the Arabia Peninsula and the eastern part of Iran by establishing two low-pressure cores above the Red Sea and the Persian Gulf and consecutive high-pressure cores above the western part of Red Sea. These storms mostly happen in the transition seasons (spring and autumn) and especially in spring. Prefrontal dust storms matched with Pattern4 in this research are formed by establishing an extensive low-pressure core above the eastern part of the Mediterranean Sea, northern part of the Arabian Peninsula, and western part of Iran. The intense performance of frontal dust storms in the Sistan Basin has also been confirmed (*Kaskaoutis et al.*, 2019). The encounter of polar jet behind the front and subtropical jet ahead created an extensive convergence, leading to the intensification of rising speed and the rise of dust from surface centers (*Wilkerson*, 1991). Such a structure has been described by *Al-Jumaily and Ibrahim* (2013) in the case study of two dust storms in Iraq.

Also, as the study of the relationship between dust estimated by the aerosol optical depth and meteorological parameters in the desert areas of Iraq, Syria, and Saudi Arabia has shown the influence of synoptic systems on the emission of dust storms in the region (*Namdari et al.*; 2018). Maps preparation of aerosol optical depth average values for each of the patterns aiming at the determination of the location of rising of dust showed that each of the patterns stimulates the most consistent synoptic dust centers in the area of Iraq, Syria, and Saudi Arabia.

References

- Abdi, H. and Williams, L.J., 2010: Principal component analysis. *Comput. Stat.* 2, 433–459.
<https://doi.org/10.1002/wics.101>
- Abdul-Wahab, S.M., Ahmad, O.A., Adel, M.A., and Mazen, E.A. 2017: Seasonal variability and synoptic characteristics of dust cases over southwestern Saudi Arabia, *Int. J. Climatol*, 38 105–124. DOI: 10.1002/joc.5164. <https://doi.org/10.1002/joc.5164>
- Alam, K., Trautmann, T., Blaschke, T., and Subhan, F., 2014: Changes in aerosol optical properties due to dust storms in the Middle East and Southwest Asia. *Remote Sens. Environ* 143, 216–227. <https://doi.org/10.1016/j.rse.2013.12.021>
- Alharbi, B.H., Maghrabi, A., and Tapper, N., 2012: The March 2009 dust event in Saudi Arabia: precursor and supportive environment, *Bull. Amer. Meteorol. Soc.* 94, 515–528. <https://doi.org/10.1175/BAMS-D-11-00118>
- Al-Jumaily, K. J. and Ibrahim, M.K., 2013: Analysis of synoptic situation for dust storms in Iraq. *Int. J. Energ. Environ.* 4, 851–858.
- Azizi, G., Shamsipoor, A.A., Miri, M., and Safarrad, T., 2012: The Synoptic-Statistical Analysis of Dust Phenomenon in the Western Half of Iran, *Ecology* 38(3) 123–134.
- Babaei Fini, O., Safarzadeh, T., and Karimi, M., 2016: Analysis and Identification of Synoptic Patterns of Dust Storms in the West of Iran, *Geograph. Environ. Hazards* 17, 105–119.
- Charlson, R.J. and Heintzenberg, J., 1995: Introduction in Aerosol Forcing of Climate. Report of the Dahlem Workshop on Aerosol Forcing of Climate, Berlin, April 24-29.
- Choobari.O.A., Zawar-Reza, P., and Sturman, A., 2014: The global distribution of mineral dust and its impacts on the climate system: a review, *Atmos. Res.* 138, 152–65. <https://doi.org/10.1016/j.atmosres.2013.11.007>
- Chun, Y.S., Boo, K.O., Kim, J., Park, S., and Lee, M., 2001: Synopsis, transport and physical characteristics of Asian dust in Korea, *J. Geophys. Res.* 106, 18461–18469. <https://doi.org/10.1029/2001JD900184>
- Ghahri, F., Ranjbar Saadatabadi, A., and Katiraei, P., 2012: Study of Meteorological Patterns and Extensive Summer Dust Production Sources in the South of Iran, *Marine Sci. Technol. Res.* 7, 1–20.
- Hsu, N.C., Tsay, S.I., King, M.D., and Herman, J.R., 2004: Aerosol properties over bright reflecting source regions, *IEEE Trans, Geosci. Remote Sens.* 42, 557–569. <https://doi.org/10.1109/TGRS.2004.824067>
- Kaiser, H.F., 1960: The application of electronic computers to factor analysis. *Educ. Psychol. Measure.* 20, 141–151. <https://doi.org/10.1177/001316446002000116>
- Kaskaoutis, D.G., Francis, D., Rashki, A., Chaboureau, J.-P., and Dumka, U.C., 2019: Atmospheric Dynamics from Synoptic to Local Scale During an Intense Frontal Dust Storm over the Sistan Basin in Winter 2019. *Geosciences* 9, 453. <https://doi.org/10.3390/geosciences9100453>
- Khoshkish, A., Alijani, B., and Hejazizadeh, Z., 2011: The Synoptic Analysis of Dust Systems in Lorestan Province, *Appl. Res. Geograph. Sci.* 18(21), 91-110.
- Kurosaki, Y. and Mikami, M., 2003: Recent frequent dust events and their relation to the surface wind in East Asia. *Geophys. Res. Lett.* 30 (14), 1736. <https://doi.org/10.1029/2003GL017261>
- Lashkari, H. and Sabouei, M., 2013: The Synoptic Analysis of Dust Storm Patterns in Khuzestan Province, *Sepehr Geographical Inform. Quart. J.* 22, No. 87, 32–38.
- Legrand, M., Plana-Fattori, A., and N'Doumé, C., 2001: Satellite detection of dust using the IR imagery of Meteosat: Infrared difference dust index, *J. Geophys. Res.*, 106, 18251–18274. <https://doi.org/10.1029/2000JD900749>
- Li, W., Wang, W., Zhou, Y., Ma, Y., Zhang, D., and Sheng, L., 2019: Occurrence and Reverse Transport of Severe Dust Storms Associated with Synoptic Weather in East Asia. *Atmosphere*, 10(1), 4. <https://doi.org/10.3390/atmos10010004>
- Mahowald, N., Albani, S., Kok, J.F., Engelstaeder, S., Scanza, R., Ward, D.S., and Flanner, M.G., 2014: The size distribution of desert dust aerosols and its impact on the Earth system, *Aeolian Res.* 15, 53–71. <https://doi.org/10.1016/j.aeolia.2013.09.002>
- Middleton, N. J., 1986: Dust storms in the Middle East. *J. Arid Environ.* 10(2), 83–96. [https://doi.org/10.1016/S0140-1963\(18\)31249-7](https://doi.org/10.1016/S0140-1963(18)31249-7)

- Monikumar, R., and Revikumar, P.V., 2012: Occurrence of widespread dust followed by thunderstorm over Qatar on 4th February 2010 – a case study, *Pakistan J. Meteorology* 9(17), 49-56.
- Namdari, S., Karimi, N., Sorooshian, A., Mohammadi, G., and Sehatkashani, S., 2018: Impacts of climate and synoptic fluctuations on dust storm activity over the Middle East. *Atmos. Environ.* 173, 265–276. <https://doi.org/10.1016/j.atmosenv.2017.11.016>
- Namdari, S., Valizade, K.K., Rasuly, A.A., and Sarraf, B.S., 2016: Spatio-temporal analysis of MODIS AOD over the western part of Iran. *Arabian J. Geosciences* 9(3), 191. <https://doi.org/10.1007/s12517-015-2029-7>
- Natsagdorj, L., Jugder, D., and Chung, Y.S., 2003: Analysis of dust storms observed in Mongolia during 1937–1999, *Atmos. Environ.* 37, 1401–1411. [https://doi.org/10.1016/S1352-2310\(02\)01023-3](https://doi.org/10.1016/S1352-2310(02)01023-3)
- Nickovic, S., Cuevas Agulló, E., Baldasano, J. M., Terradellas, E., Nakazawa, T., and Baklanov, A., 2015: Sand and Dust Storm Warning Advisory and Assessment System (SDS-WAS) Science and Implementation Plan: 2015–2020.
- Qi, Y., Ge, J., and Huang, J., 2013: Spatial and temporal distribution of MODIS and MISR aerosol optical depth over northern China and comparison with AERONET. *Chinese Sci. Bull.* 58(20), 2497–2506. <https://doi.org/10.1007/s11434-013-5678-5>
- Qian, W., Quan, L., and Shi, S., 2002: Variations of the dust storm in China and its climatic control, *J. Climate* 15, 1216–1229. [https://doi.org/10.1175/1520-0442\(2002\)015<1216:VOTDSI>2.0.CO;2](https://doi.org/10.1175/1520-0442(2002)015<1216:VOTDSI>2.0.CO;2)
- Ravi, S. and D’Odorico, P., 2005: A field-scale analysis of the dependence of wind erosion threshold velocity on air humidity, *Geophys. Res. Lett.* 32, L21404. <https://doi.org/10.1029/2005GL023675>
- Raziei, T., 2018: A precipitation regionalization and regime for Iran based on multivariate analysis. *Theor. Appl. Climatol* 131, 1429–1448. <https://doi.org/10.1007/s00704-017-2065-1>
- Sedaghat, M. and Nazaripoor, H., 2018: A New Attitude in Determining the Summer Atmosphere of Iran, *Climatol. Res.* 9, 77–88.
- Sedaghat, M., Mehrnia, S., Barzegar, S., and Zangiabadi, M.A., 2016: The Hazardous Effects of Haloxylons around Kerman City on the Formation of Aerosol's Centers, *Nat. Hazards Manage.* 3, 199–210.
- Shao, Y., and Wang, J.J., 2003: A climatology of northeast Asian dust events. *Meteorol. Zeit.* 12 187–196. <https://doi.org/10.1127/0941-2948/2003/0012-0187>
- Sun, J., Zhang, M., and Liu, T., 2001: Spatial and temporal characteristics of dust storms in China and its surrounding regions, 1901–1999: relations to source area and climate. *J. Geophys. Res.* 106, (D10), 10325–10333. <https://doi.org/10.1029/2000JD900665>
- Tegen, I, Werner, M, Harrison, S.P., and Kohfeld, K.E., 2004: Relative importance of climate and land use in determining present and future global soil dust emission, *Geophys. Res. Lett.* 31, L05105. <https://doi.org/10.1029/2003GL019216>
- Trigo, I.F., Bigg, G.R., and Davies, T.D., 2002: Climatology of cyclogenesis mechanisms in the Mediterranean, *Month. Weather Rev.* 130, 549–569. [https://doi.org/10.1175/1520-0493\(2002\)130<0549:COCMIT>2.0.CO;2](https://doi.org/10.1175/1520-0493(2002)130<0549:COCMIT>2.0.CO;2)
- Trigo, I.F., Davies, T.D., and Bigg, G.R., 1999: Objective climatology of cyclones in the Mediterranean region, *J. Climate* 12, 1685–1696. [https://doi.org/10.1175/1520-0442\(1999\)012<1685:OCOCIT>2.0.CO;2](https://doi.org/10.1175/1520-0442(1999)012<1685:OCOCIT>2.0.CO;2)
- Vali, A.A., Khamoushi, S., Mousavi, S.H., Panahi, F., and Tamaski, E., 2014: The Climatic Analysis and Tracking of Extensive Dust Storms (EDSs) in the South and Center of Iran, *Ecology* 40, 691–972.
- Wang, J.X., 2015: Mapping the global dust storm records: Review of dust data sources in supporting modeling/climate study. *Curr. Pollut. Rep.* 1, 82–94. <https://doi.org/10.1007/s40726-015-0008-y>
- Warren, S.D., 2014: Role of biological soil crusts in desert hydrology and geomorphology: implications for military training operations, *Rev. Engineer. Geology.* 22, 177–186. [https://doi.org/10.1130/2014.4122\(16\)](https://doi.org/10.1130/2014.4122(16))
- Wilkerson, W.D., 1991: Dust and forecasting in Iraq and adjoining countries, USAF Environmental Technical Applications Center, John Wiley, New York, 72p.
- World Meteorological Organization, 2013: Establishing a WMO Sand and Dust Storm Warning Advisory and Assessment System Regional Node for West Asia: Current Capabilities and Needs. *Technical Report* 1121.
- Zhou, Z.J., 2001: Blowing sand and sand storm in China in recent 45 years. *Quat. Sci.* 21, 9–17.

- Zolfaghari, H., and Abedzadeh, H., 2005: The Synoptic Analysis of Dust Systems in the West of Iran. Geograph. Develop. 3(6), 173–188.*
- Zolfaghari, H., Masoumpoor Samakoush, J., Shaygan Mehr, Sh., and Ahmadi, M., 2012: The Synoptic Study of Dust Storms in the western regions of Iran during 2005-2009 (Case Study: Extensive Wave in July 2009), Geograph. Environ.Plan. 22, 17–34.*